

# Assessment of Depth Data Acquisition Methods for Virtual Reality Mission Operations Support Tools

Alexandra Forsey-Smerek  
Massachusetts Institute of Technology  
Cambridge, MA 02139  
aforsey@mit.edu

Ferrous Ward  
Massachusetts Institute of Technology  
Cambridge, MA 02139  
ferrous@mit.edu

Lindsay Sanneman  
Massachusetts Institute of Technology  
Cambridge, MA 02139  
lindsays@mit.edu

Jennifer Heldmann  
NASA Ames Research Center  
Moffett Field, CA 94035  
jennifer.heldmann@nasa.gov

Darlene Lim  
NASA Ames Research Center  
Moffett Field, CA 94035  
darlene.lim@nasa.gov

Cody Paige  
Massachusetts Institute of Technology  
Cambridge, MA 02139  
cpaige@mit.edu

Don Derek Haddad  
Massachusetts Institute of Technology  
Cambridge, MA 02139  
ddh@mit.edu

Jessica Todd  
Massachusetts Institute of Technology  
Cambridge, MA 02139  
jetodd@mit.edu

Dava Newman  
Massachusetts Institute of Technology  
77 Massachusetts Avenue  
Cambridge, MA 02139  
dnewman@mit.edu

**Abstract**—NASA intends to be back on the Moon within the next two years, and to have long-duration, manned missions to Mars in the late 2030s. These future exploration goals demand a paradigm shift. Mission operational complexity is increasing and – with the development of heavy lift launch capabilities and increased funding of lunar orbital and surface missions – cadence of lunar missions will increase. A sustained human presence on the Moon, and eventually Mars, demands new enabling technologies and capabilities to support in situ resource utilization (ISRU).

The development of ISRU technologies requires precursory scientific and prospecting missions to identify and characterize available resources. These missions will employ robotic and human explorers to perform traverses over the lunar surface and collect data to fulfill scientific objectives. The time and monetary resources required to support a mission make maximizing the scientific return of each mission critical. Given the wide range of scientific objectives often found within a mission, the vast scope of diverse expertise within the Earth-located science team will prove invaluable to strategic decision making. Essential to maximizing scientific return on these missions is the ability of the Earth-located science team to be central to rapid science decision making, between and during traverses.

Human-computer interaction needs to lead mission planning priorities to enable rapid decision processes. Treating machines as collaboration tools allows for improved cross-team communication, improved decision-making processes, reduced task loads, and flexibility in temporal and spatial planning. Multi-user naturalistic visualization techniques can be used to analyze, discuss, and interpret near-real-time data with the potential to dramatically improve science support room situation awareness, maximizing scientific return on robotic and human exploration missions.

The virtual reality Mission Simulation System (vMSS), is a virtual reality platform designed at MIT by the Resource Exploration and Science of our Cosmic Environment (RESOURCE) team, which will provide teams with a collaboration interface for planetary exploration missions. As an early step in development of vMSS, we examine various methods to acquire depth data necessary for development of a high-resolution three-

dimensional map of the lunar surface, which will serve as a basis of the platform. In this paper we argue the importance of high-resolution depth data for scientific return, and the limitations of current planetary surface mapping tools using methods such as orbital data and Structure-from-Motion (SfM) Photogrammetry. We present a comparative analysis of four different methods to achieve depth-mapping using stereo cameras, short-range time-of-flight, LiDAR, and 360° 3D VR imagery. For this analysis, we performed a field experiment with the Boston Dynamics Spot robot, taking advantage of its ability to maneuver in geologically relevant terrain. Finally, we present planned future integration of science analysis tools based on depth imagery into vMSS, with the goal of handling the expected proliferation of real-time science data throughout science and resource prospecting missions.

## TABLE OF CONTENTS

1. INTRODUCTION.....	1
2. VR APPLICATION TO MISSION OPERATIONS .....	2
3. DEPTH DATA ACQUISITION METHODS .....	4
4. OBJECTIVES.....	5
5. CAMERA SELECTION AND EVALUATION CRITERIA	5
6. FIELD EXPERIMENT.....	6
7. INITIAL FINDINGS.....	9
8. FUTURE WORK.....	10
9. CONCLUSIONS.....	12
ACKNOWLEDGMENTS .....	13
REFERENCES .....	13
BIOGRAPHY .....	13

## 1. INTRODUCTION

NASA's comprehensive Artemis Plan describes goals to not only return astronauts to the lunar surface, but to establish a sustained human presence on the Moon. In situ resource utilization (ISRU) has been identified as a key technology to enable such sustained lunar missions [1]. ISRU technologies

can diminish astronaut reliance on Earth materials through local lunar production of such resources as fuel, water, and oxygen. The first step to enabling future ISRU technology dependent on lunar volatiles is the identification and characterization of lunar volatiles.

As stated in NASA's Plan for Sustained Lunar Exploration and Development, "Our return to the Moon begins with robots" [2]. Prior to human return to the lunar surface, robotic pioneers will conduct scientific investigation to inform location selection for human habitation and ISRU technology design. The first of NASA's lunar robotic missions, the Volatiles Investigating Polar Exploration Rover (VIPER), is slated to launch in November of 2023. The VIPER mission will explore the promising region of the Moon's South Pole, where volatile deposits may be cold trapped and maintained on the surface and subsurface [3]. The investigative nature of the prospecting mission and the unpredictability of the lunar environment create a need for rapid identification and response to discoveries during traverse, and a flexible science operations plan that enables and enhances science return from the mission. The VIPER Science Team (VST) will need to perform geological and thermal environmental statistical analyses as informed by a suite of rover instruments that will be downlinking data near real-time. This will require high levels of science team member situation awareness of the lunar surface, and rapid team convergence on a group decision. Operations software to support efficient monitoring, access, and analysis of science data and fast decision making have been identified as essential for robotic science missions [4]. While Virtual Reality (VR) will not be used for VIPER, VR has been suggested as a capability that would support similar operational conditions on forthcoming missions, including human missions [1], [5].

The Resource Exploration and Science of our Cosmic Environment (RESOURCE) team, funded by NASA's SSERVI (Solar System Exploration Research Virtual Institute), informs future ISRU through the scientific investigation of potential resources on SSERVI Target Bodies, and the development of operations and hardware associated with ISRU prospecting. The MIT branch of the RESOURCE team focuses on operations and associated technologies for optimizing human interaction with robotic explorers. The MIT RESOURCE team has demonstrated the capability of a virtual Mission Simulation System (vMSS) to provide high-throughput data integration and digital co-location in a three-dimensional virtual environment[6].

Essential to the creation of a three-dimensional surface map for integration into VR or a desktop platform is three-dimensional surface data. Current lunar surface maps available from orbital data, such as those produced by the Lunar Orbiter Laser Altimeter (LOLA) with a maximum resolution of of 10 m/pixel, or the Lunar Reconnaissance Orbiter Camera (LROC) with a resolution of 0.5 m/pixel, do not provide high enough depth data resolution for cm-scale geological data analysis. Surface maps of the Martian surface have been created using Structure-from-Motion (SfM) Photogrammetry [7]. However, hardware and processing requirements make SfM Photogrammetry an infeasible method to provide depth imagery for rapid science decision making, as demanded by future lunar missions.

In this work the MIT RESOURCE team identifies the need for a comparative analysis between different depth data acquisition methods in their ability to provide data sufficient for cm-scale geological analysis. Throughout the paper we

will refer to geological analysis, where it can be assumed we are always referring to cm-scale geological analysis. We begin by discussing the application of VR environments to future lunar mission operations, and introduce different depth data acquisition methods. We next describe the cameras we selected for assessment, and the initial evaluation criteria we are considering. We then detail a field experiment conducted to collect camera data in a simulated lunar environment using the Boston Dynamics Spot robot. Finally, we discuss initial findings and our planned next steps.

### *Related Work*

SfM Photogrammetry has been used to produce a sub-cm-scale three-dimensional outcrop model of the Martian surface using images downlinked from NASA's Curiosity Rover [7]. Integration of the model into VR has allowed scientists to traverse the Mars terrain and examine it from all angles, performing field work similar to how they might on Earth. However, the SfM Photogrammetry process is limited by strict hardware requirements, a reliance on large data sets, and an arduous alignment process to reconstruct three-dimensional point clouds. The photogrammetric process used to model the Martian surface relies most heavily on three sets of Curiosity Rover cameras: the Navcam, a pair of wide angle stereo cameras; the Mastcam, a pair of high-resolution RGB cameras; and the Mars Hand Lens Imager (MAHLI), a color, high-resolution, microscopic camera [7]. Significant camera overlap and similar optical parameters are required for straightforward terrain reconstruction. The Navcam images contain significant overlap, however only show a low level of fine-scale details. Varying focal lengths of the Mastcams result in poorly overlapping images, preventing any automation of initial image alignment. An arduous, iterative alignment process demands enormous sets of data to be integrated into point cloud generation. The first alignment step in the reconstruction of the Kimberly outcrop required 638 images from the Navcam, with the entire process requiring over 2000 total images [7]. These hardware and processing demands make SfM Photogrammetry infeasible for application to lunar robotic missions requiring rapid mapping of the lunar surface.

## **2. VR APPLICATION TO MISSION OPERATIONS**

### *Returning to the Moon*

Returning to the Moon requires reflection on lessons learned from the Apollo era, one of the most salient being the unpredictable nature of the Lunar environment. Surprises encountered during Apollo missions include the discovery of orange soil at Shorty Crater, Taurus Littrow, during Apollo-17 [8], and the collection of the Big Muley, the largest Lunar sample returned during the Apollo missions, collected during Apollo-16 on the Rim of Plum Crater in the Descartes Highlands [9]. Invaluable to both discoveries was the geologic field training of the astronauts, allowing for in situ geological analysis. Such analysis allowed for the real-time identification of unexpected regions of geologic interest, and communication of observations to provide the Science Support Room (SSR) with enough information to allow them to assist in science decision making. Future lunar robotic missions are tasked with the challenge of handling similar unforeseen circumstances, but with robotic explorers lacking the perception capabilities and prior knowledge of human explorers.

The mission operations structure of the VIPER mission and subsequent lunar robotic missions demonstrates a paradigm shift in planetary rover operations away from the structure of the more recent Mars Exploration Rover (MER) missions. The key factor driving this shift is the proximity of the Moon to Earth, presenting round-trip communication delays of only 6 to 10 seconds, a significant reduction of the 6 to 44 minute round-trip delays experienced when communicating with rovers on Mars.

The Mars Opportunity Rover operations aligned with the Martian sol so that the latest information from the rover, including images, instrument data, and state information, were downlinked at the end of the Martian day. Throughout Martian night, the mission operations team on Earth followed a tactical timeline under strict duration limits to analyze downlinked data, negotiate next steps for the robot, confirm the safety of planned next steps, and translate science plans into robot commands [10]. These plans were uplinked at the beginning of the following Martian day, during which the robot would carry out commands.

In contrast, minimal lunar communication delays allow for near-real time rover command and instrument data downlink. As opposed to the long chain of commands uplinked to the Mars Opportunity Rover at once, VIPER will be commanded step-by-step between waypoints approximately 15 feet apart. VIPER activities will include a pre-planned component, as well as a component informed based on scientific analysis during pre-planned activities [3]. For example, at a given lunar station, the locations of two out of three drill sites may be pre-selected. Scientific analysis of data downlinked during the two pre-planned drill activities will then inform the selection of the third drill site at that station. An analogue lunar volatile polar rover field campaign identified “real-time decision making based on incoming science data” as the “crux of operations” for the mission [11]. The science team thus plays an essential and enhancing role during mission operations to rapidly analyze downlinked data and make well-informed decisions about immediate next activities.

Maximizing the scientific return of imminent lunar rover exploration missions relies on maximizing the ability of the science team to accurately and efficiently make rapid decisions between and during planned traverses. Throughout this paper we refer to rapid science decision making, where “rapid” refers to a scale of 2-3 hours. The scale equates to the expected turnaround time for VIPER science decision making and similar following lunar robotic missions. The importance of maximizing scientific return in a timely manner is further pressured by potentially short lunar surface mission timelines, for example VIPER’s timeline of 100 Earth-days. Even shorter timelines are set for NASA’s Commercial Lunar Payload Services (CLPS) missions through the Payload and Research Investigations on the Surface of the Moon (PRISM) program, which are currently limited to one lunar day (7-10 Earth days). Therefore, time is of the essence for collecting the highest priority science data. The demand for optimal rapid science decision making poses two key challenges: (1) achieving a high level of science team situation awareness of the lunar surface, and (2) team convergence on a decision dependent on many types of data products and science stakeholders. VR tools have the capability to address both challenges.

#### *VR Application*

High levels of science team member situation awareness are heavily dependent on scientists achieving situation awareness

on each of Endsley’s three levels: perception, comprehension, and projection [12]. Necessary for the perception required for geological analysis are the color and depth cues available to what a geologist may have on an Earth field site. Bottom-up processing and raw feature analysis is incredibly important in the perception of the unexpected [13]. Unexplored terrain prevents the ability of top-down processing to fill in perceptual gaps with prior knowledge. This makes high-resolution color and depth imagery extremely important for the identification of unforeseen geologic points of interest. Comprehension of perceived observations requires contextual information about where observations have been made. Contextual information about the location of data collected, and the ability to visually pinpoint collection locations, has been identified as critical to remote science team situation awareness [14]. Projection describes the ability to predict future states of the current system. ISRU prospecting missions will introduce a proliferation of instrument data to be rapidly digested by science team members to inform predictions about areas of scientific relevance. Currently existing decision support tools, MoonTrek and QuickMap, use orbital data to construct a three-dimensional lunar surface map, where users can draw surface traverse paths, calculate distances, and visualize multiple data layers at once, such as elevation maps and permanently shadowed regions. However, the lunar orbital data input to these maps lacks the resolution needed to fulfill the perception requirements of geological analysis.

Converging on a science team decision does not only require individual team member situation awareness, but also a team negotiation after individuals have analyzed data products relevant to their scientific objectives. Teams possessing sufficient shared information, allowing them to build mental models of each other’s tasks and goals, have been demonstrated to perform better than teams without shared access to information [15]. A bottleneck to rapid science team decision making can be a lack of consideration of all relevant data products required to make a decision at the same time. For example, while geothermal team members and geochemical science team members may be interested in analyzing separate data sets to draw conclusions about their respective areas of interest, they must make decisions together based on the consideration of both data sets.

VR tools have the potential to improve science team situation awareness and rapid team decision making. A three-dimensional VR environment can provide the visualization of multiple layers of data products overlaid on a three-dimensional map, providing the color, depth, and contextual cues required for science team situation awareness as previously discussed. The participation of team members in the same VR environment will also allow for a shared data experience, including relevant data from all team member viewpoints. The ability for multiple team members to view the same overlaid data sets simultaneously can provide the shared information and background knowledge required for team decision making.

The MIT RESOURCE team has developed an initial set of VR mission support tools in the virtual Mission Simulation System (vMSS). Depicted in Fig.1, vMSS provides for the digital co-location of team members in a simulated mission control setting, with a table-top view of three-dimensional maps. Users have the ability to manipulate maps using handheld controls, annotate maps, and plot 3D traverses [6]. The next step of vMSS development is to include an immersive point of view, in which users are co-located at a certain

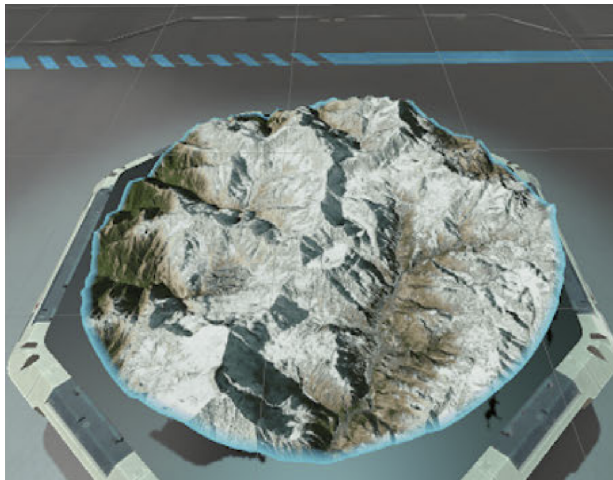


**Figure 1. 3D Tabletop view of the Himalayan Mountains displayed in vMSS.**

location within the map environment. A high-resolution immersive point of view can enable in-simulation geological and environmental analysis to promote rapid science decision making. A future development goal is to display instrument data layered over the simulated map environment, and provide supporting scientific analysis tools, such as length and volume measurement capabilities. Building an immersive virtual environment requires high-resolution imagery and depth data to supplement the low-resolution table-top view data, motivating our analysis of available depth data acquisition methods.

### 3. DEPTH DATA ACQUISITION METHODS

While SfM Photogrammetry is a proven technology, there are other available methods for depth data acquisition which could provide dramatic improvements for resolution, processing requirements, bandwidth requirements, and hardware-associated risk. SfM Photogrammetry, or stereophotogrammetry, is accomplished by overlapping images of a single scene taken from two distinct cameras. Knowing the distance between the cameras, triangulation is used to determine the depth to objects within the image. This requires two overlapping images of the complete  $360^\circ$  to render a complete depth-defined environment. Another class of depth data acquisition uses light reflection. This can be done using either structured light or time-of-flight (ToF) methods. Structured light, as the name implies, uses the distortion on an object of a known pattern of projected light to determine depth to that object. ToF interprets the time for a known pulse of laser light reflected off an object to return to a detector to determine distance to that object. In contrast to stereophotogrammetry, only a single  $360^\circ$  data set is required for the full depth-defined environment. Additionally, because there is only a single light source, the hardware placement calibration requirements needed by the dual-camera system for stereophotogrammetry are eliminated. The resolution of both reflection-based depth data acquisition techniques are dependent on the intensity of the projected light as well as the lighting within the environment. While stereophotogrammetry functions best in a brightly lit environment, the detectors of the reflection-based techniques function best with minimal interference, thus either in low light, no light, or in lighting conditions that have different wavelengths than those of the light. This would be beneficial for exploration of low-lit regions such as craters

or lava tubes. Stereo cameras, structured light, and ToF depth acquisition methods are summarized in Table 1.

While ToF cameras have long been used for large depth-of-view ( $>100$  m) depth data collection, such as for digital elevation models (DEMs), recently, commercial-off-the-shelf (COTS) shallow depth-of-view ( $<10$  m), high-resolution depth-cameras have been developed for use in the gaming and personal-use industry, such as face-recognition technology and VR games. A preliminary assessment of the technology used in these COTS parts would suggest that minimal modifications would be necessary to make them flight ready for lunar operations. The high-resolution, shallow depth of view would be particularly useful for close range geological analysis and would minimize development costs. Additionally, COTS ToF cameras may provide reductions in bandwidth requirements, improved resolution, and reduced hardware risk, in comparison to stereo cameras. Combining single layer RGB imagery with high-resolution depth data could provide a complete 3D environment with benefits over the traditional stereo camera method. We explore this technology here and assess these potential benefits.

ToF cameras have been used to map planetary surface from orbit, such as from the Lunar Orbiter Laser Altimeter (LOLA). Because of the altitude of the satellite, the data is generally lower resolution ( $> 100$  m/pixel), with some higher resolution mapping in locations of interest (10 m/pixel). The higher resolution maps are sparse, however, and require specific missions to lower the orbit of the satellite to capture. Even these higher resolution maps would not provide sufficient resolution to see cm-scale surface texture, thus making geological analysis unavailable for smaller scale features.

High-resolution (on the cm scale) DEMs for large area coverage would be data-restrictive and unnecessary, given that it is unnecessary to have cm-scale resolution at large distances from the location of analysis. Here it becomes critical to assess the resolution required, and how far out this resolution is needed. This will minimize the strength of the laser required as well as reducing bandwidth. Additionally, it is important to assess combinations of data. For instance, it would be beneficial to be able to overlay RGB data onto depth data to provide a complete image of the environment [16], [17]. Resolution of RGB imagery must also be assessed. If the data products and hardware benefits provided by ToF cameras

**Table 1. Various types of depth-cameras and their limitations and use-cases.**

Camera	Depth range	Use Cases	Space-based Limitations
Stereo cameras	Camera-placement dependent	Autonomous vehicles, Mars rover, 3D film industry.	Calibration of dual camera system, need for overlapping imagery. Suffers from occlusion.
Structured light	<10 m	3D scanners, computer vision, health care (3D reconstruction).	Limited by light emitter power, subject to occlusion.
Time-of-flight	<10 m to >100 m	Measure distance, DEMs, remote sensing, object scanning, navigation, obstacle avoidance, gesture recognition, reactive altimeters.	Limited by light emitter power and wavelength, surface albedo can cause errors.

prove to be more valuable than stereo camera methods, then the near readiness of the COTS ToF cameras can be taken advantage of for near-future lunar exploration missions.

#### 4. OBJECTIVES

Agile lunar prospecting mission operations demand the need for high levels of science team member situation awareness and rapid team decision making. VR mission operations support tools can address these challenges, however, high-fidelity VR environments hinge on high resolution depth data input. Prior depth data collection techniques via orbital data capture and Structure-from-Motion Photogrammetry are insufficient to support the demands of upcoming lunar missions for cm-scale geological data analysis.

The goal of the field experiment described is to evaluate a range of depth data types and collection techniques as input to science decision making within a VR environment. Camera data was collected in a simulated lunar landscape, and limitations of the lunar operating environment informed the selection of metrics by which to evaluate the cameras. This initial evaluation serves to identify the type of depth data and acquisition techniques most optimal for scientific analysis. The scope of this paper covers the selected cameras for assessment and evaluation criteria, and a detailed description of the field experiment. We touch on initial findings from the field experiment, and future analysis we plan to perform.

The long term objectives of the RESOURCE team are to (1) determine the optimal camera or camera combinations for VR environment data input, and (2) assess the ability to perform cm-scale geological analysis using depth imagery as compared to RGB and two-dimensional data alone.

We will use the collected experiment data to assess the depth of field, field of view, and image quality of cameras as compared to the bandwidth required to optimize their visualization capabilities. We will also assess the five cameras in the maximum and minimum lighting conditions and their ability to capture geologically relevant features. We plan to use 360 VR video collected for outreach purposes to provide a complete view of the environment with overlaid depth data.

#### 5. CAMERA SELECTION AND EVALUATION CRITERIA

##### Camera Selection

Five COTS cameras were initially selected for evaluation, in addition to the stereo cameras on board the experiment

robot. Two of each of the following types of cameras were selected: 1) stereo camera, 2) time-of-flight, and 3) VR 360 Video. Selection of each COTS camera was based on camera performance, market availability, and camera price. The Vuze 3D VR camera, one of the selected VR 360 Video cameras, was ultimately not evaluated in the field experiment, given limitations further discussed in Section 6. Detailed camera specifications on the five camera types evaluated in the field experiment can be found in Table 2. Light Detection and Ranging (LiDAR) cameras are a specific type of time-of-flight camera which were used. LiDAR uses pulsed lasers to build point clouds from which 3D images are constructed.

*Integrated Spot Cameras*—The Spot robot comes equipped with five standard cameras with global shutter. The grayscale image sensors can each provide a fisheye image, a depth image, and a depth image adjusted in the frame of reference of the fisheye image. Ideal operating range for depth images is 4m. The embedded Spot cameras were located two in the front, one on each side, and one in the back. Camera placement provided a 360° horizontal Field of View (FoV).

*Intel RealSense D435i*—The Intel RealSense D435i is a stereoscopic depth camera with an 87° horizontal FoV, a 58° vertical FoV, and up to 1280x720 depth stream output resolution at up to 90 fps. The camera module also contains an RGB camera with a 69° horizontal FoV and a 42° vertical FoV at 2 MP resolution. Ideal operating range is between 0.3 m to 3 m. An integrated IMU collects time-stamped data on camera movement and orientation to provide for more robust depth data reconstruction.

*Intel RealSense L515*—The Intel RealSense LiDAR Camera L515 is a solid state LiDAR depth camera with 70±3° horizontal FoV, a 55±3° vertical FoV, and up to 1024x768 depth stream output resolution at 30 fps. The LiDAR can achieve depth accuracy between 5 mm and 14 mm in the ideal range of .25 m to 9 m. The integrated RGB camera has a 70±3° horizontal FoV, a 43±3° vertical FoV, and 2 MP RGB resolution at 30 fps.

*Velodyne VLP-16*—The Velodyne LiDAR Puck is a LiDAR depth camera with 360° horizontal FoV and 30° vertical FoV. Angular horizontal resolution is 0.1°-0.4° and vertical angular resolution is 2°. The camera can achieve depth accuracy of ±3 cm for a measurement range of up to 100 m.

*Insta 360 ONE X*—The Insta 360 ONE X is a VR camera that can take RGB photos at 6080x3040 resolution, and RGB video with a resolution of 5.7K at 30 fps. The camera provides an immersive view with a 360° horizontal FoV and 180° vertical FoV. Additionally, the device is equipped

**Table 2. Specifications of the Boston Dynamics Spot Robot cameras and the 4 camera options mounted on the robot for the field experiment.**

Camera	Type	Field of View	Range
Integrated Spot cameras (x5)	stereo, B&W, video	360°	4m
Intel RealSense D435i	stereo, RGB, video	70°	9m
Intel RealSense L515	time-of-flight (laser), RGB, video	70°	up to 9m
Velodyne VLP-16	LiDAR (Class-1 laser)	360° (30° vertical)	100m
Insta360 One VR camera	RGB video	360° (180° vertical)	N/A

with an onboard stabilization capability, which smooths video footage and prevents the need for a gimbal.

*Vuze 3D VR*—The Vuze 3D VR camera provides an immersive view with a 360° horizontal FoV and a 180° vertical FoV through the use of eight fisheye lenses. The camera can take RGB stereoscopic photos and videos with 4k resolution per fisheye lens at 30 fps.

#### *Evaluation Criteria*

The six evaluation criteria chosen were: depth of field, field of view, resolution, bandwidth requirements, processing requirements, and lighting conditions. Camera evaluation criteria were determined through consideration of the unique limitations imposed by the lunar operating environment and associated mission operations concepts. Limitations considered included low light and directed light conditions; limited bandwidth constraints of lunar robotic missions; time delay for data transmission; and limited on-board processing capabilities. The six evaluation criteria are introduced in more detail below. These criteria by no means cover the full tradespace that should be considered when selecting a camera for lunar operations. Additional limiting factors, such as weight and power requirements, will also play a large role in selection. These criteria were selected to gain initial insight into what data types and acquisition methods would be most beneficial to conducting geological analysis, and inform future investigation into optimal camera selection. Key in evaluating these different criteria is consideration for the mission objective. For instance, when planning a long-range traverse path, one would expect a high level map with visible obstacles to be of greatest use, but when selecting sample sites based on geological points of interest, high resolution immersive maps would provide the greatest benefit. Here we focus on mission operations related to geological analysis required for scientific and prospecting missions.

*Depth of Field*—Depth of field (DOF) describes the distance between the closest and farthest objects that are of acceptably sharp focus in an image. This metric is often described as the camera’s optimal operating range. The DOF required for scientific analysis will likely differ from mission to mission, depending on scientific objectives, terrain type, and the robot’s ability to position itself in relation to areas of interest.

*Field of View*—Field of view (FoV) describes the maximum area that a camera can image. It is dependent on both the focal length of the lens and the size of the sensor. Horizontal FoV and vertical FoV are measured in degrees, describing the horizontal and vertical envelopes of view from the camera lens. FoV will dictate how much environmental area a scientist will be able to view at once. It will be important to analyze the required size for appropriate scientist situation awareness and contextual information when performing scientific analysis.

*Resolution*—Camera resolution describes the size of the produced image in terms of the number of pixels the image contains. It is typically reported as image width in pixels by image height in pixels (W×H). Higher resolution means more pixel information, resulting in a high quality, crisp image. Resolution will determine the level of detail scientists are able to discern from one image. It is important to determine the minimum level of resolution required to perform scientific analysis, given the resolution of an image directly corresponds to the size of the image file. A balance must be struck between image resolution and image file size, which will be inherently restricted by bandwidth requirements.

*Bandwidth Requirements*—Bandwidth describes the amount of data that can be sent over a connection in a given period of time. Bandwidth is typically measured by a factor of bits per second. The size of the data produced by each camera type determines the bandwidth demand of the camera for data downlink.

*Processing Requirements*—We introduce the criteria of processing to describe the speed and ease of the integration of data into a format that would support scientific analysis. We include this metric as a way to contrast arduous integration processes, such as those encountered by SfM Photogrammetry, and seamless VR integration processes, such as the insertion of 360 VR camera footage into a VR environment. This evaluation metric will need further development to assess, given techniques are not yet formalized for the integration of data from each camera into the VR environment. This assessment will be an area of future work.

*Lighting Conditions*—The cameras were assessed under daytime and nighttime lighting conditions. Under nighttime conditions, a single source overhead spotlight was directed toward the traverse path in order to simulate lunar daytime lighting. Under daytime conditions, data was collected to contrast the baseline performance of the cameras under terrestrial daytime lighting with camera performance under simulated lunar daytime lighting. The complete darkness necessary to replicate lunar night lighting was not achievable in the field experiment environment. Simulating lunar lighting conditions can help to expose the limitations of RGB cameras, and the necessity for depth cameras to supplement colored images when regions of interest are not illuminated.

## 6. FIELD EXPERIMENT

A two-day field experiment was carried out on a granitic beach with exposed bedrock in Marblehead, MA, in order to assess the chosen cameras over the selected evaluation criteria. Six traverses were carried out over the two days; four under nighttime conditions and two under daytime conditions. Camera payloads were mounted on top of a Boston Dynamics

Spot robot and data was remotely accessed throughout the traverse.

### Hardware

**Cameras**—Five out of the six cameras selected were evaluated in the field experiment. The Vuze 3D VR camera was ultimately not studied in the field experiment, given inherent camera limitations. The camera lacks a built in stabilization system, which results in shaky footage when mounted to a robot without a gimbal. Additionally, the Software Development Kit (SDK) for live streaming the Vuze 3D camera can only work when connected to a Windows 10 PC through proprietary software that requires serial key activation. In contrast, the Insta360 line of 360° cameras are able to stream through mobile devices or any other operating system. The Insta360 ONE X uses both Bluetooth Low Energy (BLE) and WiFi to connect to a mobile device, making it ideal for real-time monitoring. Therefore, the Insta360 ONE X was selected to be used as the sole VR camera.

**Spot Robot**—The Boston Dynamics Spot robot was chosen as the roving vehicle, upon which payloads were mounted. Spot's ability to traverse unstable and uneven terrain enabled us to traverse a site that resembled challenging lunar terrain with geologically relevant points of interest. Spot can be teleoperated via a tablet provided by Boston Dynamics, or via laptop commands using the WASD keyboard keys. Spot can act as its own WiFi access point, allowing for easy remote connection and control from a laptop.

The SpotCORE computer, an additional computer provided by Boston Dynamics for developer payload integration, mounts to the top of Spot. Primary interface with the SpotCORE computer was provided via wifi networking through the Spot access point and USB connectivity. Power was provided by onboard batteries external to Spot, and passed through to the SpotCORE computer. SpotCORE provided a simple power interface for our payloads and a location to implement required payload software. WiFi access to Spot allowed us to remotely access SpotCORE to monitor and record payload data. Remote operations were critical to collecting realistic data along a traverse path with multiple data-collection waypoints.

### Site Selection

A site was selected to fulfill the following criteria of exposed bedrock; unstable terrain; identifiable geological features; accessibility, describing access to power and wifi, and within walking distance to the street for heavy equipment transport; and availability during both daytime and nighttime. The site selected was in Marblehead, MA on a private beach with low tides allowing for up to 4 hours of accessibility at one time. The beach contained exposed bedrock of granitic rock with quartz veining. Marblehead is within the Avalon Belt geologic province. The Avalonian terrane is a dense granite exposed 14,000 years ago with the retreat of the Laurentide Ice Cap. The quartz veins within the granite are indicative of the high heat, high pressure accretionary emplacement of the Avalonian terrane onto proto-North America during the closing of the Iapetus Ocean in the Devonian period.

### Traverse Plan

The traverse plan shown in Fig.3 was selected with waypoints an average of 3 m apart given the lowest DOF was 4 m for the integrated Spot stereo cameras. Some waypoints were placed closer together to capture points of interest and a single waypoint (W06, Fig.3) was placed in a challenging region to

demonstrate the robot's capabilities to navigate uneven, rocky terrain, as well as demonstrate the benefits of capturing 360° FoV for a distinct location off of the traverse path.

Two geologic points of interest were selected at W04 and W06 to assess each camera's ability to capture color-specific and geometry-specific geologic information. At W04 distinct 90-degree fracture angles in the granitic rock were identified (Fig. 4), hypothesized to be identifiable by depth data. At W06, continuous, visible quartz veining throughout the rock was identified (Fig. 5), demonstrating a geologic point of interest requiring color differentiation.

### Data Collection Methodology

**Spot traverse control**—Spot was controlled from either the handheld tablet provided by Boston Dynamics, or from a laptop computer using WASD controls. Control type depended on the type of data being collected. In order to collect data from the Spot stereo cameras, a laptop needed to be connected and commanding Spot. If data was not being collected from the Spot stereo cameras for a given traverse, the handheld tablet was used. To control spot using WASD keyboard controls the Boston Dynamics `wasd.py` script was used from the Spot SDK.

**Spot stereo cameras**—Two python scripts were developed to collect images from the five spot stereo cameras. The Spot SDK provided a sample script titled `get_image.py` which took arguments of camera names and image types, and collected data of that type for that specific camera when called. This script was adapted in order to prevent having to pass in each camera type and each data type as arguments at every collection point. The adapted script took in arguments of "front" or "back", to either collect all data types from either the two front and two side cameras, or to collect all data types from the back camera. Two argument options were required because the Spot image service was unable to handle all data types being requested from all five cameras at once.

A second python script was written to efficiently gather data at each set of waypoints along a traverse. The goals of the script were to ensure only one script call was necessary for each traverse; to allow users to uniquely label each waypoint; and to inform the user when image collection was complete at a waypoint. The script first prompted users to input where they would like to save the traverse data. Next, the script prompted users to input the name of a waypoint. Once users entered a name, the script would run the adapted `get_image.py` script twice, capturing stereo camera data for all cameras on Spot. Once this process was done the script would report that data capture at the waypoint was complete, and would wait for the input of the next waypoint name. A separate folder for each waypoint was created. Each folder contained the fifteen images captured at that waypoint, three for each of five cameras.

**Velodyne LiDAR**—The VeloView software was installed on SpotCORE to operate and record data for the Velodyne camera. The software was set-up to forward the LiDAR data to a secondary computer through the VeloView GUI. This preliminary setup was only required upon initial setup of the software, after which the VeloView data was accessible on the secondary computer. Two data set types were taken for the Velodyne LiDAR: a continuous recording of a full traverse and a recording of each waypoint for a complete traverse. The waypoint recordings were captured for  $5 \pm 2$  seconds at each waypoint and were trimmed to a single frame of data for final analysis.

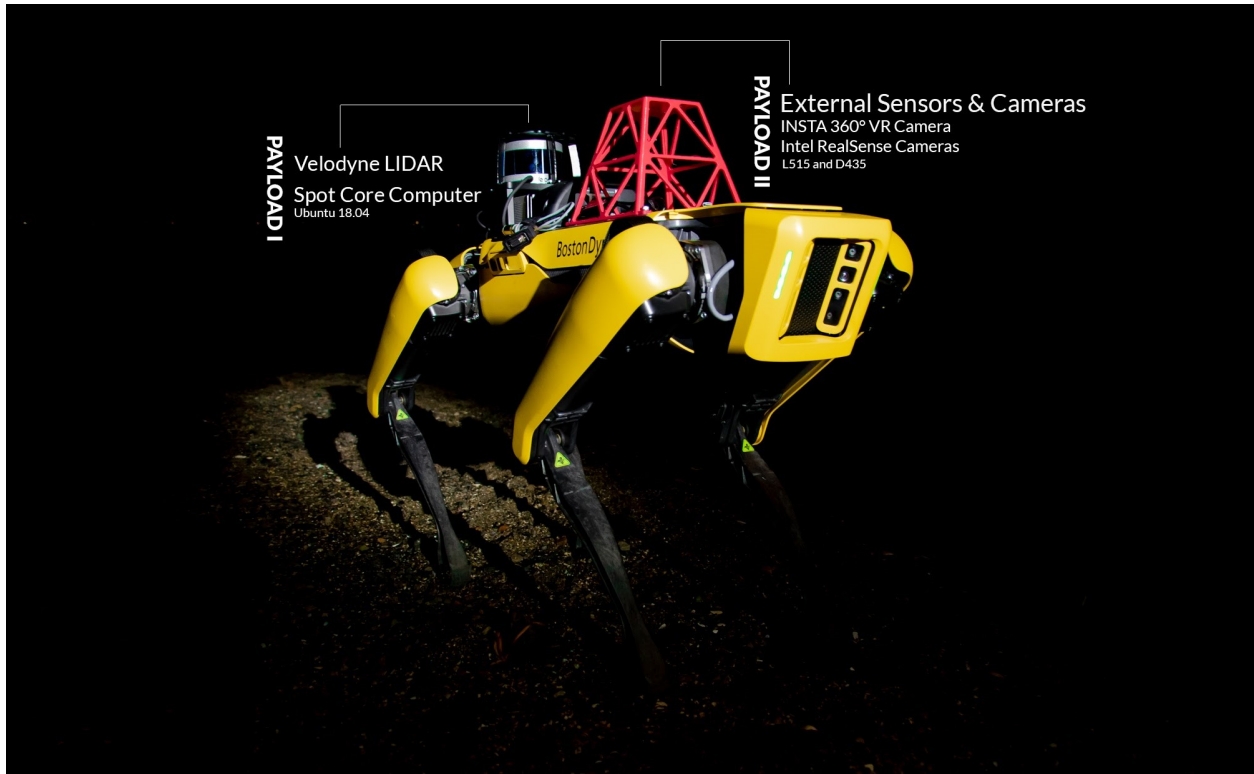


**Figure 2. Boston Dynamics Spot robot photographed in nighttime conditions with single spotlight lighting. Payload I consists of the Spot Core Computer and Velodyne LiDAR. Payload II carried either both Intel RealSense Cameras or the Insta 360 VR camera on the custom payload tower.**



**Figure 3. Overhead image of selected traverse and location of thirteen waypoints.**

*Intel RealSense L515 and D435i*—The RealSense Viewer software was installed on SpotCORE and accessed via ssh

to control and capture data for the two Intel RealSense cameras. At each waypoint the camera was activated on the





**Figure 4. Waypoint 4 (W04): Granatic rock with fracturing. Quarter placed for size.**



**Figure 5. Waypoint 6 (W06): Quartz veining in granite. Quarter placed for size.**

RealSense Viewer software GUI, a recording was started for the waypoint using a prespecified naming convention, and the camera (either L515 or D435i) was manually rotated 360°. The first camera was then deactivated and the second camera (whichever was not activated previously) was activated. The recording was started and the second camera was rotated 360°. This was repeated for each waypoint.

*Insta360 ONE X*—Data was accessible remotely on a phone application. Data was collected as a single continuous recording of a full traverse.

#### *Experimental Procedure*

*Payload Registration*—The SpotCORE Ubuntu computer provided by Boston Dynamics for payload integration was mounted on the rear of the Spot robot and registered on Spot as SpotCORE with no LiDAR through the Spot GUI. The SpotCORE can be set up with an integrated Velodyne LiDAR, which allows the Spot software access to the LiDAR data for use of the automation features. When used for this feature, the LiDAR is captured with a lower point-cloud density and is not accessible by other software interfaces, such as VeloView, the software provided by Velodyne to capture LiDAR data. In order to bypass this use case, SpotCORE must be registered without LiDAR.

The Velodyne puck was mounted in a protective casing on the rear of the Spot robot just behind the SpotCORE (Payload I

in Fig.2). This was registered separately from SpotCORE as a LiDAR imaging device, and therefore did not speak to Spot. Registration of the puck was done through the Spot GUI only to provide mass balance data to Spot. Power was provided by Spot. Both RealSense cameras were mounted together on a custom payload in the mid-section of the Spot robot (Payload II in Fig.2). These were registered as a single mounted payload using their combined weight within the Spot GUI. Power was provided by Spot. The Insta360 camera was mounted on the custom payload tower when the RealSense cameras were not in use (Payload II in Fig.2).

*Traverse Schedule*—The field experiment took place over the span of two days. The first day, three traverses were completed under nighttime conditions. The first traverse was designed with multiple spotlights for VR demonstration purposes, and was not representative of lunar day lighting. Insta 360 and continuous Velodyne LiDAR data types were captured. The second traverse was designed with a single source spotlight, representative of lunar day lighting. Again Insta 360 and continuous Velodyne LiDAR data types were captured for VR demonstration. The third traverse also used a single source spotlight to simulate lunar day lighting. Velodyne LiDAR and Spot stereo camera data were captured at each waypoint for depth data analysis.

The second day, two traverses were completed under daytime conditions, and one traverse was completed under nighttime conditions. The first daytime traverse collected data for VR demonstration purposes, capturing Insta360 and continuous Velodyne LiDAR data. The second daytime traverse collected data for depth data analysis, capturing Velodyne LiDAR, Intel RealSense D435i and L515, and Spot stereo camera data at each waypoint. The nighttime traverse was executed with a single source spotlight, representative of lunar day lighting. Intel RealSense D435i and L515 data was captured at each waypoint.

## 7. INITIAL FINDINGS

### *Field of View and Depth of Field*

The Intel RealSense cameras and the integrated spot cameras all had limited fields of view. For the integrated spot camera this was mitigated by having 5 separate cameras, which combined, provided a full 360° FoV. The Intel RealSense cameras were instead rotated 360° to capture the complete 360° FoV. This will result in larger processing requirements and will necessitate some overlap for stitching in these cameras. The Velodyne and Insta 360 cameras intrinsically captured the 360° FoV. The DOF for the stereo cameras and RGB imagery was dependent on the lighting conditions, while the ToF cameras rely on their internal laser power. The Intel RealSense cameras both had limited DOF (<9 m), while the Velodyne had up to 100 m DOF. For the application of geological analysis, the Velodyne's large DOF was not necessary and the loss of resolution due to this large DOF, in fact, was a hindrance.

### *Resolution*

Selecting a camera specifically for geological analysis implies a need for higher resolution data in the near-FoV. Table 3 lists the resolution for all of the cameras (RGB and depth data), however, here we focus specifically on the resolution of the depth data. The resolution of the Velodyne, Table 3, is defined as an angle. It is based on the LiDAR's capture of 300,000 points/s, and is dependent on the distance to an

object, decreasing in density by the distance squared to the object. Despite the large number of points captured in the Velodyne point-cloud, the viewing distance available reduces the resolution dramatically compared to the L515. This is evident in Fig. 6 showing the left-side view (with respect to Spot) of waypoint 6. The uppermost image shows the Velodyne point-cloud, with Spot highlighted by the red box. The lower images show the stereo-depth data (D435i on the lower left) and the near-view ToF data (L515 on the lower right), both of which have much higher resolution depth data. Comparing the D435i and the L515 we can see that for similar resolution, we can achieve a more detailed surface texture with the ToF data.

**Table 3. Comparison of camera resolutions.**

Camera	Data type	Resolution
Integrated Spot cameras (x5)	B&W image	424 x 240
Integrated Spot cameras (x5)	stereo-depth	424 x 240
Intel RealSense D435i	RGB	1920 x 1080
Intel RealSense D435i	stereo-depth	1280 x 720
Intel RealSense L515	RGB	1920 x 1080
Intel RealSense L515	ToF	1024 x 768
Velodyne VLP-16	ToF	Horizontal - 2°

#### Bandwidth requirements

Because each of the different cameras uses a different file type and recording technique, the data required some initial processing to provide an accurate comparison of the file sizes. Table 4 shows the file type, file size and reduced file size for each of the different depth data cameras for a single waypoint; this does not include the Insta 360 ONE X as it is a continuous video stream of RGB video only.

For the integrated spot cameras, the only data reduction necessary was to select the depth data image from a single waypoint folder, eliminating the fisheye and visual frame images. For the two Intel RealSense cameras, the data was captured at each waypoint as a continuous 360° video. Since the camera captures 70° in a single frame, with 5° of overlap for image stitching, snapshots were saved every 60° as ply files containing both the RGB and depth data. These were saved as human-readable binary files (ply) without meshing using the RealSense Viewer software. The reduced size for each waypoint was the sum of the six snapshots. The Velodyne data used here was the single waypoint capture. The total size indicates the full 5 seconds of video taken allowing the point-cloud to stabilize, while the reduced size is a single snapshot of the data at the end of the video.

All but the Velodyne camera are a combination of either RGB or B&W with depth data (either stereo-depth or ToF). Here we see that while we are using different file types and so cannot infer any absolute conclusions, the combination RGB with ToF data (L515) would pose the largest bandwidth requirements. While the Velodyne has much smaller file sizes, we must consider that this does not include any RGB data, and the point-cloud density is not sufficient for geological feature identification.

#### Varying in lighting conditions

Fig. 6 is a nighttime capture of waypoint 6. RGB imagery was lower resolution in the nighttime lighting condition than in the daytime lighting condition. Although we would expect the ToF cameras to outperform the stereo cameras at night, we found that both cameras provide similar depth data in both daytime and nighttime lighting conditions. Given the stereo cameras use the RGB imagery to determine the depth data, this is a surprising result and requires more testing to determine why the depth data from the stereo cameras function in low-light despite low RGB image resolution.

## 8. FUTURE WORK

### Depth Camera Analysis

Following this experiment, we will incorporate our findings for optimal depth data collection for geological analysis into a Science Analogue experiment, along with scale visualization and measurement tools. This future round of testing will assess a data pipeline development, camera selection, and tool development. These will be assessed for a geologically relevant task, such as identifying stratigraphic sequences or characteristics (cross-bedding, ripples, mud-cracks, inclusions, etc.). Users with geological field work experience will be asked to assess the optimal characteristics of each camera to compare the different approaches. Moving forward, we will be replacing the Intel RealSense L515 with the Microsoft Azure Kinect, as the RealSense line is being discontinued.

### Depth Camera Flight Readiness

We will do a preliminary assessment of the Azure Kinect for flight readiness as a COTS payload. This will include environmental testing: vibration, vacuum and temperature, as well as minor hardware modifications to the electronics and power components for integration into a Commercial Lunar Payload System (CLPS) rover. The high-level flight readiness testing and assessment plan is outlined in Table 5. One of the key developments for use of a depth-camera on a lunar mission will be the data pipeline. We will need to further assess bandwidth requirements, data processing sequences and locations (processing on the rover vs. transmitting raw data), and where in the pipeline the data will be most usefully accessed for different applications. A conceptual data pipeline is shown in Fig. 7.

The bandwidth requirement for the Azure Kinect is shown in Table 6. Consideration for reducing the bandwidth will be made during further field experiments and human in the loop testing. We will use this data to design our data pipeline and assess where in this pipeline the data should be transmitted (minimizing transmission bandwidth) and where it should be integrated into a desktop application or a VR application.

As part of the consideration for the data pipeline and bandwidth requirements we will also assess if any of the processing would need to be done on board the rover. The full rendering of a depth-map from the Microsoft Azure Kinect camera requires a minimal host compute of a Jetson Nano server. This will provide the baseline for the maximum processing power requirement for full rendering on board the rover.

### VR Environment and Tool Development

We will continue to develop the fundamental vMSS platform with further hardware testing, VR platform development,

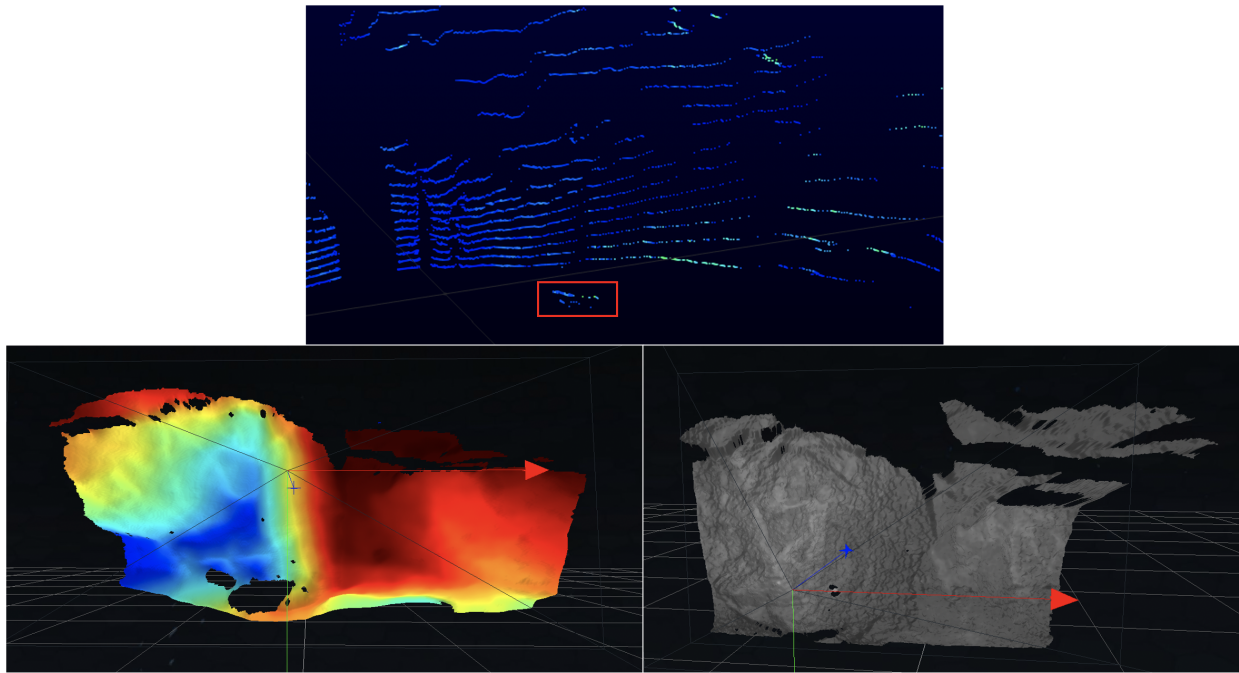


Figure 6. Comparison of depth data from the Velodyne VLP16 (top), Intel RealSense D435i (lower left) and Intel RealSense L515 (lower right) at waypoint 6.

Table 4. File type, file size (total and reduced) for each camera.

Camera	File Type	Total Size	Reduced Size
Integrated Spot cameras (x5)	png	1.2 MB	1.09 MB
Intel RealSense D435i	ply	4.33 GB	7.975 MB
Intel RealSense L515	ply	2.57 GB	21.35 MB
Velodyne VLP-16	pcap	2.84 MB	0.78 MB

Table 5. COTS Microsoft Azure Depth-Camera flight readiness testing and assessment plan - details on vacuum pressure and temperature requirements to be provided by Tony Colaprete, NASA Ames.

Test Type	Plan	Requirements and Location
Vibration table	Open COTS part, stake down parts and add supports where failure occurs	NASA Ames - one day on shake 3-axis shake table
Vacuum testing	1-week in vacuum, then remove and power on (prelim testing). Then 1-week in high-vacuum, assess any parts that may impact vacuum	Prelim - MIT, High-vacuum - NASA Ames
Thermal testing	Prepare for need to provide heating on rover - thermal heat tape tests	NASA Ames and MIT- test power requirements of heat tape
Laser function	Assess the visibility of having the field of view in the rover's shadow to avoid increasing laser power	MIT field testing - varying ground reflectivity and light source angles
Power supply	Modify to 28 V power regulated by rover - meet 5V at 6 W to meet camera peak power draw	MIT in collaboration with Microsoft - hardware modification
Data rates	Rover maximum data transmission rates are 54 Mbps, lossless compression from camera is 42.2 Mbps - need to minimize data transmission	MIT - part of pipeline design

multi-modal environmental overlays, and performance testing. Going beyond initial assessments of data acquisition, we also intend to quantitatively assess data quality for visual representations in VR and for scientific analysis.

Once the depth data collection technique has been selected, scientific tool development will begin on the three-dimensional model within vMSS. The primary tool set currently under development is based around distance mea-

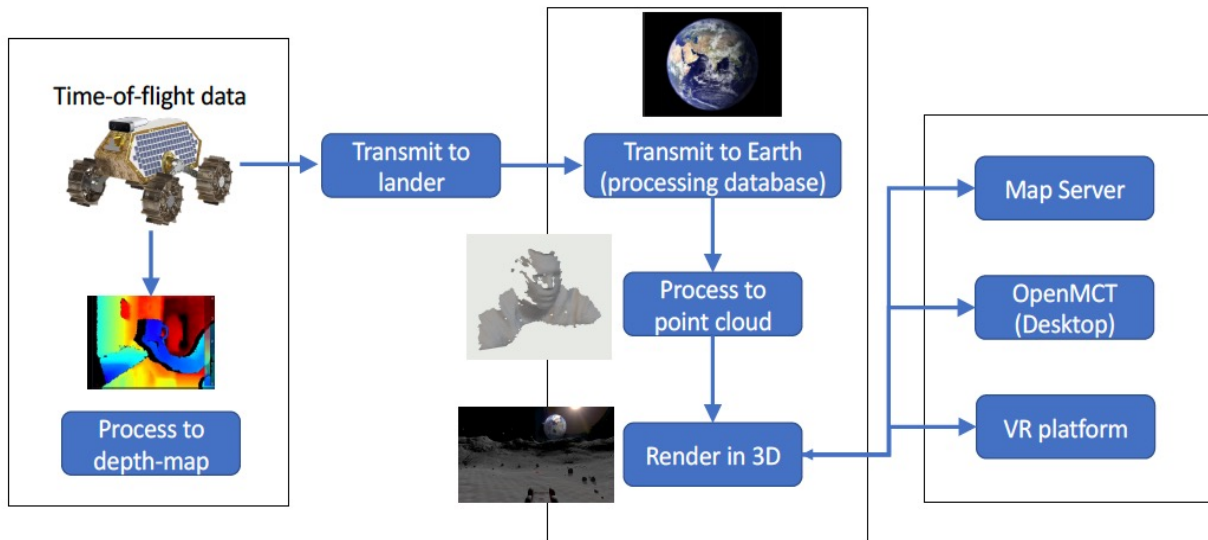


Figure 7. Conceptual data pipeline of a depth-camera onboard a lunar rover for use with multiple applications.

Table 6. Microsoft Azure Depth-Camera bandwidths provided by Microsoft team.

Resolution	Compression Type	Bandwidth
Native	None	1 Mpixel peak
	Lossless	42.2 Mbps
Binned	None	10 Mbps
	Compression	5 Mbps or less

measurements from a user-placed set of points, such as in Fig. 8. Here, a user places an arbitrary set of points, defining an object in 2D or 3D. This analytical tool can then use those annotated points to determine distance, angle, and area through a closed polyline. Fig. 9 shows a conceptual image of the user-interface for the 3D use case. This methodology would be most useful in situations where accurate cm-scale volume and area measurements are required for scientific analysis.

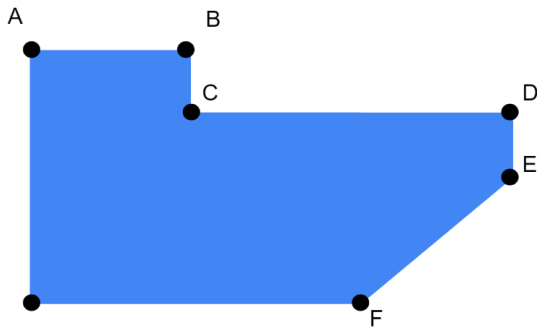


Figure 8. High level overview of user mesh generated object used for performing measurements of distance, angle, area, and volume.

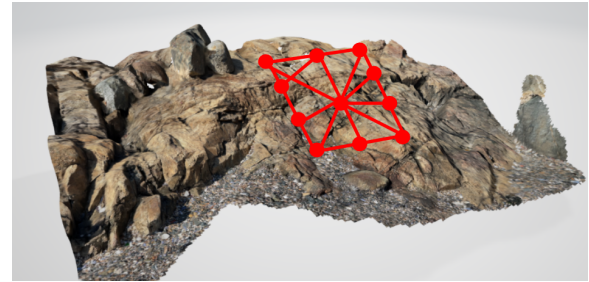


Figure 9. Conceptual overview of user-placed point grid over collected data, with an automated mesh.

## 9. CONCLUSIONS

Future lunar robotic missions will rely heavily on rapid science team decision making to fulfill mission objectives and maximize science return. VR mission operations support tools can enable rapid science geological analysis and team decision making by improving science team member situation awareness of the lunar environment and team convergence on a decision. The MIT RESOURCE team has demonstrated the capabilities of a VR environment to visualize three dimensional terrain through the development of vMSS. The basis for lunar VR mission operations support tools will be a high-fidelity three-dimensional map of the lunar surface region of interest. We examine the performance of five cameras, including three different camera types (stereo, ToF, and 360 VR) to be integrated onboard future lunar robotic missions as data providers for such VR mission operation support tools. Initial evaluation suggests short-range ToF depth imagery accompanied with RGB imagery can provide both detailed surface texture imaging and color imaging, which may be sufficient for cm-scale geological analysis. However, bandwidth requirements may still be a limiting factor, and further VR environment integration and analogue testing will be required to ultimately select the optimal camera for supporting mission scientific objectives. Future work will focus on final camera selection and VR environment development, including visualization and analysis tools.

## ACKNOWLEDGMENTS

We would like to thank Boston Dynamics for their support in our project efforts. Boston Dynamics loaned us the Spot robot and provided invaluable help when integrating our camera payloads. We would also like to acknowledge SSERVI and the RESOURCE project which funded this work.

## REFERENCES

- [1] NASA, “Artemis plan: Nasa’s lunar exploration program overview,” 2020.
- [2] —, “Nasa’s plan for sustained lunar exploration and development,” 2020.
- [3] —, “Volatiles investigating polar exploration rover proposal information package,” 2021.
- [4] K. Hambuchen, J. Marquez, and T. Fong, “A review of nasa human-robot interaction in space,” *Current Robotics Reports*, vol. 2, no. 3, p. 265–272, 2021.
- [5] K. H. Beaton, S. P. Chappell, A. Menzies, V. Luo, S. Y. Kim-Castet, D. Newman, J. Hoffman, J. Norheim, E. Anandapadmanaban, S. P. Abercrombie *et al.*, “Mission enhancing capabilities for science-driven exploration extravehicular activity derived from the nasa basalt research program,” *Planetary and Space Science*, vol. 193, p. 105003, 2020.
- [6] F. Ward, T. Piercy, J. Heldmann, D. Lim, A. Colaprete, A. Cook, and D. Newman, “A virtual reality mission simulation system (vmss) supporting closed-loop mission control,” in *50th International Conference on Environmental Systems*, no. ICES-2021-257, July 2021.
- [7] G. Caravaca, S. L. Mouelic, N. Mangold, J. L’Haridon, L. L. Deit, and M. Masse, “3d digital outcrop model reconstruction of the kimerley outcrop (gale crater, mars) and its integration into virtual reality for simulated geological analysis,” *Planetary and Space Science*, vol. 182, p. 104808, 2020.
- [8] E. M. Jones, “The apollo 17 lunar surface journal,” Los Alamos National Lab., NM (United States), Tech. Rep., 1995.
- [9] D. Stoeffler, S. Schulien, and R. Ostertag, “Big muley 61016: Multiphase shock and crystallization history of a composite troctolitic-anorthositic rock,” in *Lunar and Planetary Science Conference*, vol. 6, 1975.
- [10] Z. Mirmalek, *Making time on Mars*. MIT Press, 2020.
- [11] J. L. Heldmann, A. Colaprete, R. C. Elphic, G. Mattes, K. Ennico, E. Fritzler, M. M. Marinova, R. McMurray, S. Morse, T. L. Roush *et al.*, “Real-time science operations to support a lunar polar volatiles rover mission,” *Advances in Space Research*, vol. 55, no. 10, pp. 2427–2437, 2015.
- [12] M. R. Endsley, “Toward a theory of situation awareness in dynamic systems,” *Human Factors: The Journal of the Human Factors and Ergonomics Society*, vol. 37, no. 1, p. 32–64, 1995.
- [13] C. D. Wickens, S. E. Gordon, Y. Liu, and J. Lee, *An introduction to human factors engineering*. Pearson Prentice Hall Upper Saddle River, NJ, 2004, vol. 2.
- [14] L. Turchi, S. J. Payler, F. Sauro, R. Pozzobon, M. Masironi, and L. Bessone, “The electronic fieldbook: A system for supporting distributed field science operations during astronaut training and human planetary exploration,” *Planetary and Space Science*, vol. 197, p. 105164, 2021.
- [15] C. A. Bolstad and M. R. Endsley, “Shared mental models and shared displays: An empirical evaluation of team performance,” *Proceedings of the Human Factors and Ergonomics Society Annual Meeting*, vol. 43, no. 3, p. 213–217, 1999.
- [16] C. Beder, B. Barctczak, and R. Koch, “A comparison of pmd-cameras and stereo-vision for the task of surface reconstruction using patchlets,” in *IEEE Conference on Computer Vision and Pattern Recognition*, 2007, pp. 1–8.
- [17] K.-D. Kuhnert and M. Stommel, “Fusion of stereo-camera and pmd-camera data for real-time suited precise 3d environment reconstruction,” in *IEEE/RSJ International Conference on Intelligent Robots and Systems*, IEEE, Ed., 2006, pp. 4780–4785.

## BIOGRAPHY



**Alexandra Forsey-Smerek** is a Master’s student in Aerospace Engineering at MIT and is a member of the Human Systems Lab. She received a Bachelor’s degree in Aerospace Engineering from MIT in 2020. Her current research is focused on methods to promote appropriate human trust calibration throughout human robot interaction.



**Cody Paige** received her B.A.Sc in Engineering Physics in 2008 from Queen’s University, Canada. She received her M.A.Sc. in Aerospace Engineering from the University of Toronto, Canada in 2010. She is concurrently completing a Ph.D. at Dalhousie University, Canada in Earth Science with a focus on geochronology as well as a Ph.D. in Aeronautics and Astronautics from MIT with a focus on enabling a permanent human presence on the Moon.



**Ferrous Ward** received his B.S.E. in Biomedical Engineering in 2017, and his M.S.E. in Biomedical Engineering in 2017 from the University of Michigan. He is currently completing a Ph.D in Aeronautics and Astronautics from MIT, focusing on enhancing science operations for future exploration missions.



**Don Derek Haddad** is an MIT PhD candidate in Media Arts and Sciences at MIT and is a member of the Media Lab's Responsive Environment Group. He received his Master's degree in Media Arts and Sciences from MIT in 2017. Don's current research is focused on HCI, extending to the fields of wearable computing, ambient technologies, smart textile and fashion, and space exploration.



**Dr Dava Newman** is the Director of the MIT Media Lab and the Apollo Program Professor of Astronautics at MIT and a Harvard-MIT Health, Sciences, and Technology faculty member. She served as NASA Deputy Administrator, the first female engineer in this role, from 2015–2017. Her research and teaching include aerospace biomedical engineering, humans becoming interplanetary, advanced suit design, leadership development, innovation and policy.



**Lindsay Sanneman** is a Ph.D candidate in the Department of Aeronautics and Astronautics at MIT and is a member of the Interactive Robotics Group in the Computer Science and Artificial Intelligence Laboratory. She received a Bachelor's degree in Aeronautics and Astronautics from MIT in 2014 and a Master's degree in Mechanical Engineering from MIT in 2018. Her current research is focused on the application of explainable AI to human-machine collaborative contexts such as the AI value alignment setting.

focused on the application of explainable AI to human-machine collaborative contexts such as the AI value alignment setting.



**Jessica Todd** is a Ph.D. Student at the Massachusetts Institute of Technology and the Woods Hole Oceanographic Institute. Her research is primarily in autonomous scientific robots for planetary and ocean exploration, with a focus on adaptive autonomous exploration, informative path planning, and perception. She completed her M.S. in Aeronautics from the Massachusetts Institute of Technology in 2019, and a B. E. in Aeronautical (Space) Engineering and a B.S. in Physics from the University of Sydney in 2016. Outside of her Ph.D, Jessica is also a Controls and Integration & Test Engineer for the MIT Self-Assembling Lunar Tower Project.

technology in 2019, and a B. E. in Aeronautical (Space) Engineering and a B.S. in Physics from the University of Sydney in 2016. Outside of her Ph.D, Jessica is also a Controls and Integration & Test Engineer for the MIT Self-Assembling Lunar Tower Project.



**Jennifer Heldmann** received her Ph.D in Planetary Science from the University of Colorado at Boulder. She is now at the NASA Ames Research Center studying recent water on Mars and planning future human exploration to the Red Planet. Jennifer has extensive experience participating in research and field campaigns to enable human and robotic exploration of the Solar System.

She is the Principal Investigator for NASA's FINESSE and RESOURCE projects.



**Darlene Lim** received her Ph.D from the University of Toronto during which she conducted climate change research in the Canadian High Arctic. She is now at the NASA Ames Research Center, and her work as a geobiologist has since extended to include the development of operations concepts and capabilities in support of human-robotic scientific exploration. Darlene has spent over two

decades leading field research and is the Principal Investigator of the SUBSEA and BASALT programs. She is the Deputy Project Scientist for the NASA VIPER Lunar Rover Mission.